# Characterization of a Polymer Film Optical Fiber Hydrophone for Use in the Range 1 to 20 MHz: A Comparison with PVDF Needle and Membrane Hydrophones

Paul C. Beard, Andrew M. Hurrell, and Tim N. Mills

***Abstract*—A small aperture wideband ultrasonic optical fiber hydrophone is described. The transduction mechanism is based on the detection of acoustically induced changes in the optical thickness of a 25-$\mu$m thick Parylene polymer film acting as a low finesse Fabry Perot (FP) interferometer that is deposited directly onto the end of a single mode optical fiber. The acoustic performance compares favorably with that of PVDF needle and membrane hydrophones with a peak noise-equivalent-pressure (without signal averaging) of 10 kPa over a 25-MHz measurement bandwidth, a wideband response to 20 MHz, and a near omnidirectional performance at 10 MHz. The dynamic range was 60 dB with an upper limit of linear detection of 11 MPa and a temporal stability of $< 5\%$ over a period of 20 h. The hydrophone can also measure temperature changes with a resolution of 0.065°C, offering the prospect of making simultaneous acoustic pressure and temperature measurements. The transduction parameters of the FP sensing element were measured, yielding an ultrasonic acoustic phase sensitivity of 0.075 rad/MPa and a temperature phase sensitivity of 0.077 rad/°C. The ability to achieve high acoustic sensitivity with small element sizes and to repeatably fabricate rugged sensor downleads using polymer deposition techniques suggests that this type of hydrophone can provide a practical alternative to piezoelectric hydrophone technology.**

## I. Introduction

For the measurement of broadband ultrasound fields in water, an ultrasonic hydrophone must fulfill several fundamental specifications. It should be of adequate sensitivity, broad banded with well-behaved frequency and phase response characteristics, temporally stable, and of wide dynamic range. Additionally, and perhaps most importantly, the acoustically sensitive element should be small in relation to the acoustic wavelength to avoid errors caused by spatial averaging and to provide an omnidirectional response. While hydrophones based on piezoelectric PVDF sensing elements, such as PVDF needle and membrane hydrophones, can fulfill most of these requirements, a fundamental limitation arises from the difficulty in obtaining adequate acoustic sensitivity with the small ($<$100 $\mu$m) element sizes required for low directional sensitivity at megahertz frequencies. Additionally, the sensitivity of piezoelectric hydrophones to EMI can present difficulties in the measurement of CW fields. Their fragility and expense can also make them unsuitable for the measurement of high amplitude signals and use in hostile environments.

Various optical fiber methods of ultrasound detection have been explored to address these limitations. Intrinsic optical fiber ultrasound sensors configure a length of the optical fiber itself as the acoustically sensitive element and employ interferometric [1] or polarimetric [2] methods or in fiber Bragg gratings [3] to detect acoustically induced strains within the fiber. The use of a fused silica optical fiber as a wideband, high fidelity ultrasound sensing element, however, is less than ideal. First, the high Young's modulus of fused silica results in small acoustically induced strains. Thus, to obtain adequate sensitivity, a long fiber interaction length is required, perhaps by winding the fiber into a coil [4], [5], thereby making it difficult to achieve an acoustically small element size. Second, the large acoustic impedance mismatch of fused silica to water is not conducive to achieving a wideband uniform frequency response. Intrinsic optical fiber ultrasound sensors, therefore, tend to be more applicable to the detection than quantitative measurement of a broadband field.

More promising, particularly in terms of element size, are extrinsic optical fiber sensors in which the fiber is used to deliver light to and from an optical sensor at the end of the fiber. Because the lateral dimensions of the sensitive element are defined by the spot size of the incident illumination, very small element sizes, down to the optical diffraction limit of a few microns can, in principle, be achieved. Perhaps the simplest approach is based on the detection of pressure-induced changes in the Fresnel reflection coefficient at the tip of an optical fiber [6]. Low sensitivity, however, tends to limit its application to the measurement of temporally stable signals that can be averaged over long periods or the output of high amplitude sources, such as shockwave lithotripters. More useful detection sensitivities have been achieved using interferometric methods to detect acoustically induced displacements

Manuscript received July 19, 1999; accepted Sept. 19, 1999. This project was carried out in collaboration with Precision Acoustics Ltd., UK and funded under the EPSRC/LINK Photonics Programme.

P. C. Beard and T. N. Mills are with the Department of Medical Physics and Bioengineering, University College London, London WC1E 6JA, UK (e-mail: p.beard@medphys.ucl.ac.uk).

A. M. Hurrell is with Precision Acoustics Ltd., Dorchester, Dorset DT1 1PY, UK.

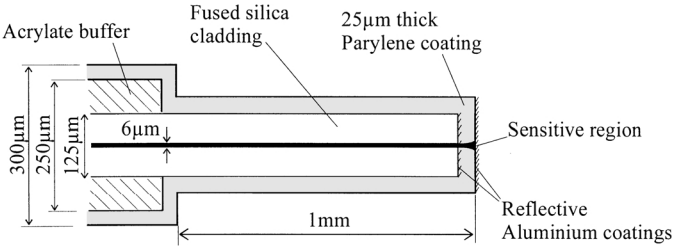


Fig. 1. Schematic of optical fiber sensor head. The black region represents the light path.

of a thin membrane [7], [8] or a fiber tip [9] or changes in the optical thickness of a solid FP interferometer. The latter approach has been implemented using a multilayer dielectric stack acting as a high finesse FP interference filter deposited on the end of an optical fiber [10]. The use of a thin polymer film as a FP interferometer for the detection of ultrasound has also been explored [11]–[14].

The advantage of this approach is that the low Youngs modulus of polymers results in acoustically induced phase shifts that are sufficiently large to provide a sensitivity comparable with that of PVDF transducers even when using a low finesse FP configuration [12]. Additionally, the well-matched acoustic impedance of polymers to water offers an intrinsically wideband response. The concept has been used to realize a miniature wideband ultrasonic hydrophone probe by bonding discrete PET (polyethylene terepthalate) FP sensing elements to the tip of a multimode optical fiber [15]–[17]. There are, however, significant limitations associated with this method of fabrication. It is time-consuming and, because of the small dimensions involved, difficult to obtain repeatedly the sub-5-$\mu$m adhesive layer thicknesses [13] between the polymer film and the optical fiber that are required to avoid significantly degrading the frequency response.

In this paper, we describe an approach that overcomes these difficulties by depositing the polymer film sensing element directly onto the tip of a single mode optical fiber using a vacuum deposition technique. Details of the sensor head and interrogation system are described in Section II. A key objective was to establish whether this type of hydrophone could provide a practical alternative to the current state of the art in piezoelectric hydrophone technology. Accordingly, a thorough analysis of the acoustic performance of the sensor and its comparison with PVDF needle and membrane hydrophones has been carried out and is described in Section III.

## II. Optical Fiber Hydrophone System

Fig. 1 shows a schematic of the sensing head. The FP sensing cavity consists of a 25-$\mu$m thick Parylene film deposited on to the plane cleaved end of a single mode optical fiber from which the final 1 mm of the acrylate buffer coating had been removed. Parylene is a polymer that can be deposited directly from the gas phase [18] to form a thin transparent film with the necessarily high degree of thickness uniformity and surface finish for it to act as an effective FP cavity. Reflective coatings, formed by the flash evaporation of aluminium, provide the mirrors of the FP cavity. The first mirror, which is deposited on to the bare cleaved end of the fiber prior to the deposition of the Parylene layer, is partially transmissive with a reflection coefficient of approximately 8%. The second mirror, which is deposited on to the Parylene layer, is fully opaque with a reflection coefficient of 70%. The low reflectivity of the first mirror coupled with the high absorption of aluminium coatings [19] ensures that the cavity is of low finesse [13].

The system shown in Fig. 2 is used to interrogate the sensor. The collimated output of an optically isolated 850-nm tunable DBR laser diode is launched into the input port of a 50/50 $2 \times 2$ fused optical fiber coupler. The connectorized sensor downlead is inserted into one output port of the coupler while the other output port is connected to a photodiode $P_L$ and used to monitor the laser power launched into the coupler. The second coupler input port is connected to the detector unit, which consists of a 25-MHz silicon pin photodiode with integral transimpedance amplifier and an external 50-$\Omega$ line driving amplifier. The FP cavity is interrogated using a simple manually controlled active homodyne scheme [13], [20]. The phase bias of the interferometer is adjusted optimally so that it lies half way between a maximum and minimum of the interferometer transfer function, the so-called quadrature point. Control of the phase bias is achieved by thermally tuning the laser diode wavelength by adjusting the current supplied to an internal Peltier element located within the laser diode package.

## III. Acoustic Characterization Set-Up

To measure the sensitivity, directivity, and linearity of the optical fiber hydrophone, an acoustic field generated by nonlinear propagation in water was used as a broadband ultrasound source. This approach is based on a hydrophone calibration technique [21] developed by the National Physical Laboratory (NPL), UK, and relies on the finite amplitude distortion of a high amplitude, 23-cycle, 1-MHz acoustic toneburst emitted by a 1.5" PZT transducer. As the sinusoidal signal propagates away from the transducer, it evolves into a sawtooth shape "shocked" waveform with a broadband frequency content composed of discrete harmonics spaced at 1-MHz intervals, typically extending to 50 MHz. The large diameter of the source transducer produces a relatively wide uniform field, +/− 0.1 dB over a 5-mm beamwidth at 20 MHz at a distance of 50 cm from the transducer. Therefore, it avoids the need for excessively high alignment accuracy, particularly for directivity measurements for which alignment to the axis of rotation is a difficult and time-consuming procedure. A computer-controlled scanning stage that allowed independent translations in X, Y, and Z directions and rotation about the

vertical axis was used to position the optical fiber hydrophones. To measure frequency response, a photoacoustic source was used (as described in [13]), which relies on the generation of short pulses of broadband ultrasound by the absorption of nanosecond laser pulses in an ink absorber [13]. For the sensitivity, frequency response, and linearity measurements, an NPL-calibrated PVDF membrane hydrophone was used as the reference hydrophone.

Intercomparisons are made with three types of PVDF hydrophones. A 50-$\mu$m thick bilaminar PVDF membrane type hydrophone [22] (Marconi Y-34-3598; GEC Marconi Ltd., Great Baddow, UK) of active element diameter 0.5 mm and two PVDF needle type hydrophones, one of active element diameter 0.2 mm (Precision Acoustics HPM02/1; Precision Acoustics Ltd., Dorchester, UK) and the other 0.075-mm diameter (Precision Acoustics HPM075/1; Precision Acoustics Ltd.). The thickness of the PVDF elements used in the needle hydrophones was 9 $\mu$m. The needle hydrophones incorporated a submersible pre-amplifier with a nominal voltage gain of 8 dB, output noise voltage of 0.1 mv (rms) over a 100-MHz measurement bandwidth, and 50-$\Omega$ output impedance.

## IV. Characterization

The transfer function of the FP interferometer is described in Section IV, A. In Sections IV, B through E, the acoustic performance, namely, the sensitivity, linearity, frequency response, and directional response, of the optical fiber hydrophone and its comparison with PVDF needle and membrane hydrophones, is discussed. Section IV, F evaluates the temperature sensitivity and its implications for stability and making simultaneous pressure and temperature measurements. Section IV, G discusses the sensor stability to establish the typical long- and short-term calibration stability that can be achieved. Unless otherwise stated, all measurements reported in this section were obtained using sensor downleads employing a 25-$\mu$m thick FP sensing film.

### A. Interferometer Transfer Function

The interferometer transfer function (ITF) describes the relationship between the DC optical power output $I_R$ of the interferometer and the optical phase difference caused by the path length difference within the cavity. It provides a means of understanding the operation of the sensor and obtaining parameters such as the acoustic phase sensitivity, linear operating range, cavity finesse, and the wavelength tuning range requirements of the laser source.

The ITF can be obtained by thermally or mechanically straining the cavity to vary the optical phase or, alternatively, by adjusting the laser wavelength $\lambda$. The latter approach was used to observe the ITF of a sensor that employed a 50-$\mu$m thick Parylene sensing film. With a 25-$\mu$m film, it was not always possible to observe a turning point of the transfer function because of the limited wavelength tuning range of the laser diode ($\sim$2 nm).

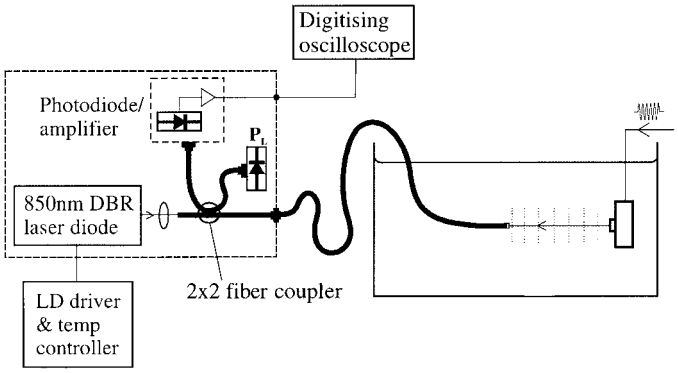


Fig. 2. Experimental set-up.

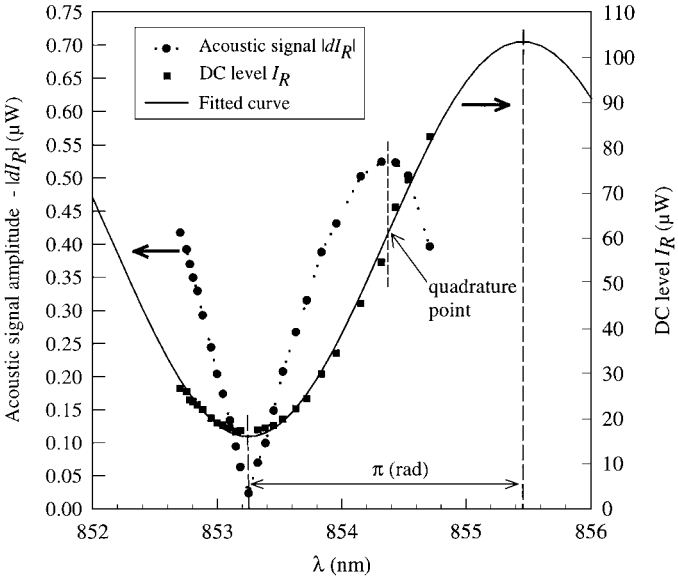


Fig. 3. Interferometer transfer function obtained by monitoring the DC optical power output $I_R$ as a function of laser wavelength $\lambda$ for an optical fiber hydrophone employing a 50-$\mu$m thick Parylene FP sensing cavity. The curve fitted to the experimental data is a cosine function. Also shown is the corresponding intensity modulation signal $|dI_R|$ caused by a 0.075-MPa acoustic signal as a function of $\lambda$.

The transfer function ($I_R$ versus $\lambda$) is shown in Fig. 3. The fitted cosine is in excellent agreement with the experimental data demonstrating the low finesse nature of the interferometer. Also shown is the simultaneous measurement of the magnitude of the sensor output $|dI_R|$ in response to a pulsed 3.5-MHz, 0.075-MPa acoustic signal as a function of $\lambda$. Note that it is the magnitude of the acoustic signal $|dI_R|$ that is plotted in Fig. 3. The signal is actually of opposite sign on either side of the ITF minimum. As expected, $|dI_R|$ is the first derivative of the transfer function; its maximum coincides with the point of maximum slope on the transfer function, the quadrature point. The maximum value of $dI_R$ lies almost exactly half way between the transfer function maximum predicted

TABLE I
NOISE EQUIVALENT PRESSURES (NEP) OF THE OPTICAL FIBER, PVDF MEMBRANE, AND NEEDLE HYDROPHONES. NO SIGNAL AVERAGING WAS USED.

| Hydrophone | Peak NEP kPa (25-MHz measurement bandwidth) |
|---|---|
| 0.5-mm diameter PVDF membrane hydrophone | 5 |
| 0.2-mm diameter PVDF membrane hydrophone | 3 |
| 0.075-mm diameter PVDF membrane hydrophone | 55 |
| Optical fiber hydrophone | 10 |

by the fitted curve and the experimentally observed minimum, demonstrating the validity of fitting to predict the ITF in this way.

Assuming a $\pi$ phase shift between the maximum and minimum of the transfer function, the horizontal axis now can be calibrated in units of optical phase. Given that the peak positive pressure of the acoustic signal is known, the acoustic phase sensitivity, defined as the optical phase shift per unit of acoustic pressure in the low frequency limit [13], can, therefore, be calculated. The acoustic phase sensitivity provides a useful comparative figure of merit because it is independent of the ITF, depending only on the sensing film optical thickness, elastic and photoelastic properties, backing configuration, and laser wavelength [13]. In conjunction with the ITF, it also enables the linearity to be estimated as described in Section IV, C. For the 50-$\mu$m thick, rigid-backed Parylene sensor for which the transfer function is shown in Fig. 3, the acoustic phase sensitivity was found to be 0.15 rad/MPa. For the water-backed benchmark configuration defined in [13], this reduces to approximately 0.075 rad/MPa, comparable with the 0.1 rad/MPa value previously obtained for PET [13]. Acoustic phase sensitivity scales with sensor film thickness, so, for the optical fiber hydrophones employing a 25-$\mu$m thick Parylene sensing film, the acoustic phase sensitivity is 0.075 rad/MPa.

### *B. Sensitivity*

The sensitivity of the optical fiber hydrophone was obtained by direct comparison of its output (as measured by an oscilloscope) with that of a calibrated PVDF membrane hydrophone in response to an acoustic signal. Corresponding waveforms were also measured using the PVDF needle hydrophones; measurements of the shocked toneburst field (Section III) by the optical fiber hydrophone and a 0.075-mm PVDF needle hydrophone are shown in Fig. 4, for example. The peak noise equivalent acoustic pressure of the optical fiber hydrophone is listed alongside those of the 0.2- and 0.075-mm PVDF needle hydrophones and a 0.5-mm membrane hydrophone in Table I. No signal averaging was used for these measurements. The output of the submersible preamp (Section III) used with the needle

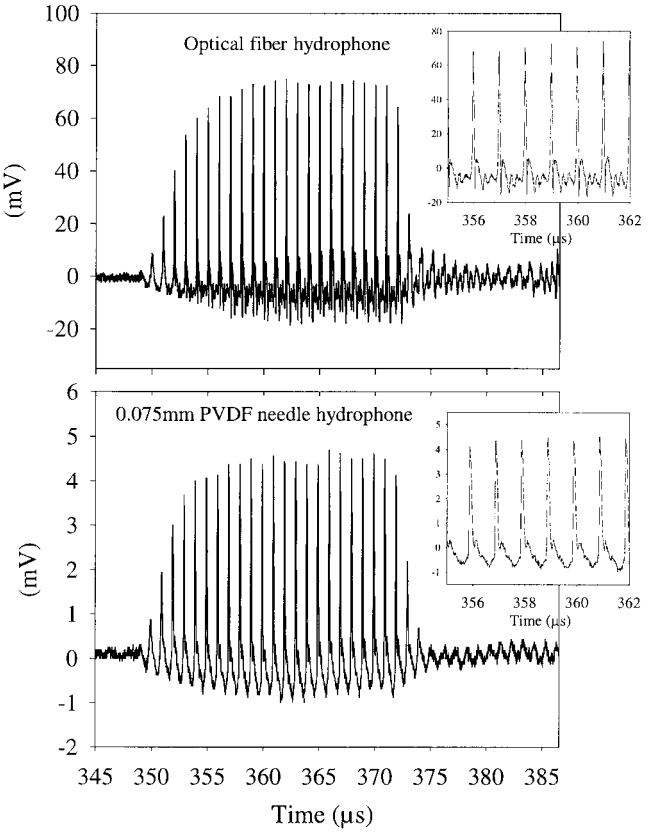


Fig. 4. Comparisons of optical fiber hydrophone output (top) with that of a 0.075-mm PVDF needle hydrophone (bottom) in response to a "shocked" 1-MHz toneburst. Insets show expanded timescale. No signal averaging was used.

hydrophones was connected to the 50-$\Omega$ input of the oscilloscope. No amplification was used with the membrane hydrophone, which was connected directly to the 1-M$\Omega$ input of the oscilloscope. For both types of PVDF hydrophone, the noise was dominated by that of the oscilloscope amplifier.

The results in Table I indicate that, for these measurement conditions, the typical detection sensitivity of the optical fiber hydrophone is likely to be a factor of two to three lower than that of a typical PVDF hydrophone with an active diameter a few hundred microns or more but significantly higher than one of sub-100-$\mu$m diameter.

### *C. Linearity and Dynamic Range*

To measure linearity, the optical fiber hydrophone was set at quadrature and positioned a few millimeters behind the PVDF membrane hydrophone. The peak-peak amplitudes of the 1-MHz fundamental of the shocked field registered by both devices as a function of the source transducer drive voltage were measured simultaneously. To obtain the true acoustic pressure arriving at the tip of the optical fiber, a correction taking into account the attenuation of the membrane hydrophone was applied. Fig. 5 shows the measured optical fiber hydrophone output as a function of acoustic pressure.

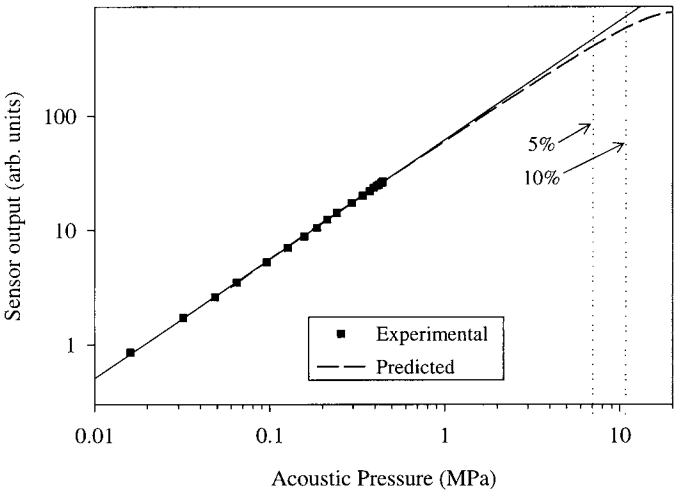


Fig. 5. Linearity of optical fiber hydrophone employing a 25-$\mu$m thick Parylene sensing film. Graph shows predicted and experimentally measured output as a function of acoustic pressure at 1 MHz. The bold line is a straight line fit to the experimental data. The dashed line is the predicted output based on the assumption of an acoustic phase sensitivity of 0.075 rad/MPa and a low finesse FP cavity. The dotted vertical lines show the acoustic pressure at which the sensor nonlinearity becomes 5 and 10%.

The sensor shows excellent linearity to 0.5 MPa. Limitations on the maximum drive voltage of the transducer meant that it was not possible to go beyond this pressure and approach the nonlinear region of the transfer function in order to make a direct measurement of the upper limit of linear response. However, it is possible to make a well-founded quantitative estimate with knowledge of the acoustic phase sensitivity and the form of the ITF. We know from the sinusoidal shape of Fig. 3 that the interferometer is of low finesse. Thus, at quadrature, acoustically induced phase shifts of up to 0.5 rad can be resolved with a linearity of better than 5%. Converting to acoustic pressure using the figure for acoustic phase sensitivity for a rigid-backed, 25-$\mu$m thick Parylene sensing film (0.075 rad/MPa) calculated in Section IV, A, we can expect linear operation to around 7 MPa. If a reduced linearity of 10% can be tolerated, an upper limit of 11 MPa and a dynamic range of 60 dB will be obtained. It is upon these considerations that the curve representing the predicted sensor output shown in Fig. 5 is based. While it would be difficult to approach the estimated 100-MPa upper limit of operation of PVDF devices [23], increased linearity could be achieved by proportionately decreasing the sensing film thickness to reduce the acoustic phase sensitivity.

### *D. Frequency Response*

To determine the frequency response, the output of the photoacoustic source [13] was measured first with the optical fiber hydrophone and then, at the same point in the field, with a calibrated PVDF membrane reference hydrophone. By comparing the discrete Fourier transforms of the time domain waveforms measured by each device and applying corrections to take into account the frequency response characteristics of the photodiode and the membrane hydrophone, the frequency response was obtained. The normalized frequency responses for four nominally identical optical fiber hydrophones are shown in Fig. 6(a), demonstrating good repeatability. The frequency responses for the PVDF membrane and needle hydrophones are shown in Fig. 6(b).

Two mechanisms contribute to the optical fiber hydrophone frequency response characteristics. The first is the spatial variation of acoustic pressure across the thickness of the sensing film caused by the incident acoustic wave and its reflection from the fused silica backing of the optical fiber. By itself, this produces a frequency response that gradually increases from zero to a small maximum at the $\lambda/4$ thickness mode resonance of the film at 22 MHz (speed of sound in Parylene = 2200 m/s) and thereafter decreasing to zero at 44 MHz. Superimposed on this are features caused by diffraction effects, the second mechanism. For a probe-type hydrophone, these tend to dominate and are responsible for the low frequency fall-off in sensitivity [24], [25] below 5 MHz observed in Fig. 6(a) and higher frequency features, most noticeably those at 14 and 17 MHz. The higher frequency features can be explained by considering the output of the sensor to be the sum of the incident plane wave and the phase-inverted cylindrical edge waves that arise from the diffraction of the plane wave around the edge of the fiber [26]. The edge wave component is time delayed with respect to the plane wave because the former has to travel from the outside edge of the fiber to the 6-$\mu$m diameter, acoustically sensitive region in the center. The resulting phase difference between the two components is dependent on frequency and, therefore, so is the sensor output. Because the small active element size (6 $\mu$m) enables the orthogonally propagating edge waves to be registered at frequencies at tens of megahertz, periodic features produced by this mechanism appear across the full extent of the thickness-mode resonance, limited sensor bandwidth. This is in contrast to the response of the 0.2-mm PVDF needle hydrophone in Fig. 6(b), which, beyond the first diffraction maximum at 3 MHz, exhibits a near uniform frequency response. The more directional response of the relatively large PVDF element size effectively bandlimits the orthogonally propagating edge waves at high frequencies, suppressing diffraction-related artifacts and allowing the well-behaved thickness-mode frequency response characteristics to dominate. Thus, for a probe-type hydrophone, regardless of the sensing mechanism, the combination of both small element size and uniform frequency response is unlikely to be achieved unless the influence of the edge waves can be suppressed in some way, perhaps by modifying the probe tip geometry.

### *E. Directional Response*

The directional responses of the optical fiber hydrophone and the PVDF needle hydrophones at 1-MHz intervals to 20 MHz were obtained by rotating each device through 180° in steps of 3.6° in the shocked field de-

scribed in Section III. The measured responses at 1, 3, 5, and 10 MHz are shown in Fig. 7. The directional response of the 0.5-mm membrane hydrophone, obtained from previously reported measurements of the effective radii as a function of frequency [27], is also shown.

By fitting the first-order Bessel function of the angular response of a circular plane piston in a rigid baffle [28] to the experimental data, the effective radii of the needle and optical fiber hydrophones as a function of frequency were obtained. These are plotted in Fig. 8 along with the effective radius of the membrane hydrophone [27]. For the PVDF hydrophones, the effective radius initially falls with increasing frequency, leveling out at a value close to the physical radius of the active element. For the optical fiber hydrophone, the effective radius also falls with frequency to a minimum at 10 MHz, where the directional response is almost flat. It has been suggested that a decrease in effective radius with frequency is characteristic of a circular receiver whose sensitive region does not fall sharply to zero around the perimeter [29]. For spot-poled PVDF receivers, such as the membrane hydrophone, this may be due to a gradual decrease in piezoelectric sensitivity around the edges of the sensitive region. Similarly, the Gaussian nature of the light distribution emerging from the single mode fiber that defines the acoustically sensitive region of the optical fiber hydrophone may also result in an apodized response. Additionally, acoustically induced deformations from outside the illuminated area could provide a contribution to the hydrophone output that results in an apodized sensitivity profile. For the needle hydrophones, apodization may occur due to edge effects such as variations in the thickness and flatness of the PVDF element near the perimeter.

Beyond 10 MHz, the directional characteristics of the optical fiber hydrophone were observed to become increasingly nonuniform with large fluctuations in amplitude and phase, and, unlike the PVDF hydrophone responses, it was no longer possible to fit the plane piston model to the data to obtain meaningful values of the effective radius. Nonuniformities in the directional response were found to be largest around 14 MHz, the location of the first diffraction minimum in the frequency response at normal incidence [Fig. 6(a)]. The magnitude of this feature is related to the degree of symmetry in the obstacle that the fiber presents to the incident field. At normal incidence, the edge waves from each point around the edge of the fiber arrive simultaneously at the center, and their contribution to the sensor output is a maximum. As the angle of incidence is increased, the symmetry is broken, the edge waves no longer arrive at the center simultaneously, and their influence on the sensor output is reduced. Thus, as the fiber is rotated, the sensor exhibits a strong angle-dependent response at frequencies that correspond to diffraction features in the normally incident frequency response. As with frequency response, it would be desirable to suppress the influence of the edge waves to obtain a well-behaved directional response at higher frequencies.

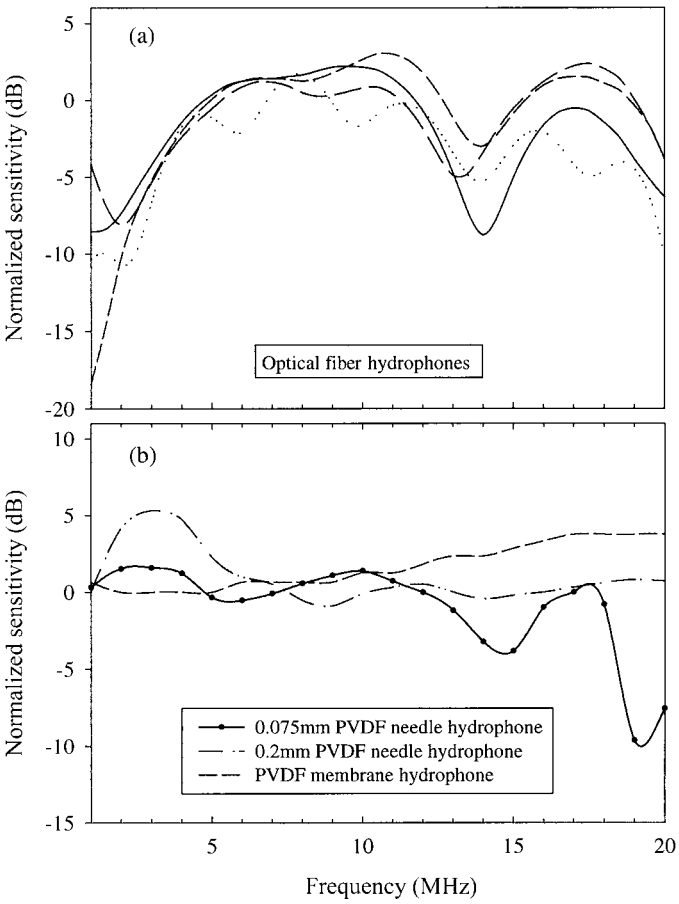


Fig. 6. Frequency responses of a) four nominally identical optical fiber hydrophones and b) PVDF needle and membrane hydrophones.

### *F. Temperature Sensitivity*

The effect of temperature variations is to change the optical thickness of the FP cavity. The key parameter is the temperature phase sensitivity, defined as the optical phase shift per unit of temperature change. It enables assessment of the temperature range over which the sensor can be operated before adjustment of the laser wavelength is required to return the interferometer to quadrature to maintain constant acoustic sensitivity. If the sensor is to be used to make measurements of temperature as well as acoustic pressure, perhaps for investigating ultrasound-induced heating effects in biological tissues, it enables the temperature resolution and linear operating range to be determined.

To obtain the temperature phase sensitivity, the sensor output was compared with that of a reference thermocouple while in a temperature-controlled water bath. By varying the temperature so that a maximum and minimum of the interferometer transfer function could be observed, a temperature transfer function, analogous to the wavelength transfer function in Fig. 3, was obtained. From this, the temperature phase sensitivity was calculated to be 0.077 rad/°C, comparable with that of PET [30]. Thus, for a quadrature set optical fiber hydrophone, a temperature change of 13°C would be required to produce a 10%

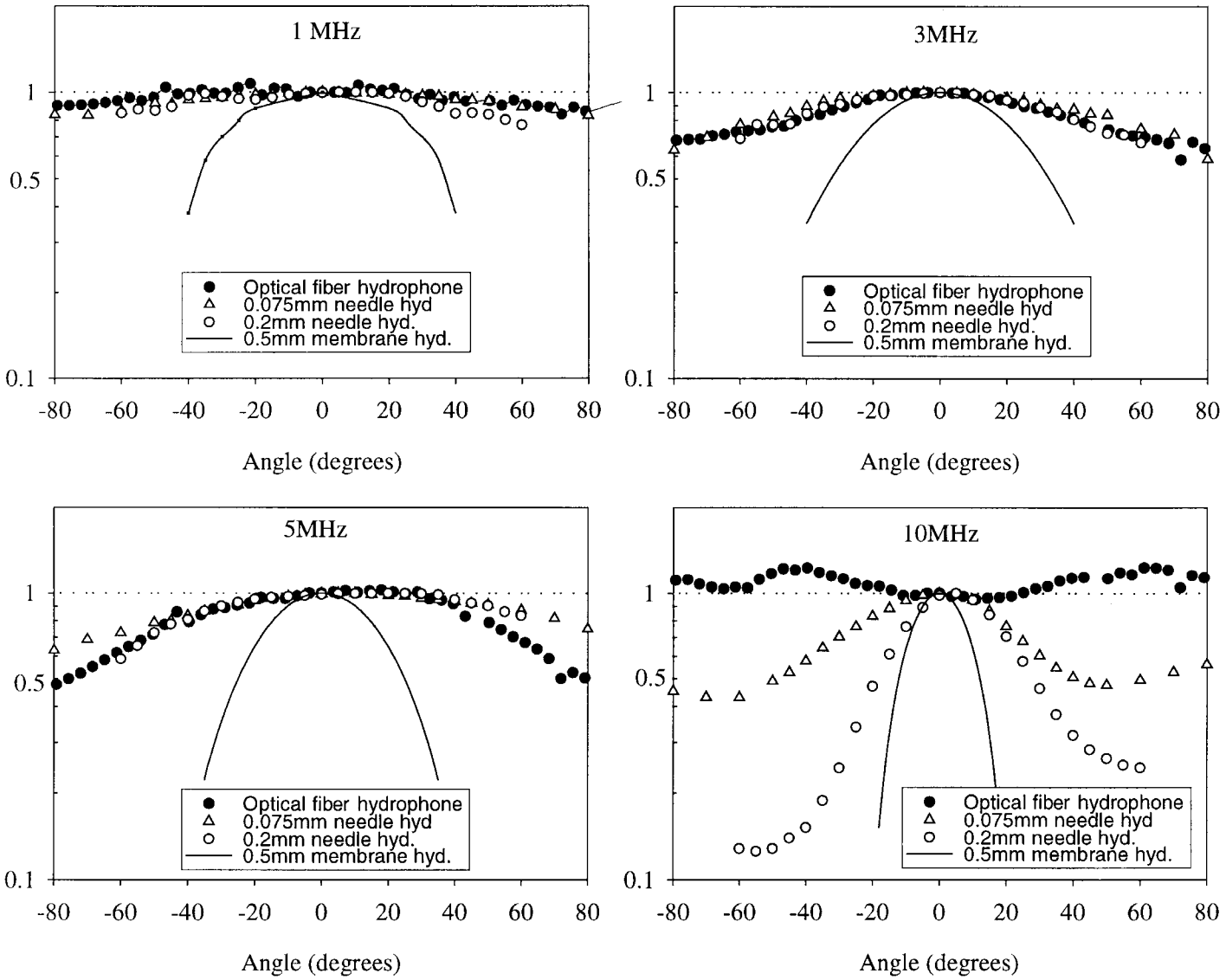


Fig. 7. Comparison of directional responses of optical fiber hydrophone with PVDF needle and membrane hydrophones at 1, 3, 5, and 10 MHz.

change in the acoustic sensitivity. The noise equivalent temperature was found to be 65 mK over a 25-MHz measurement bandwidth. Because the sensor was operated well below the detector saturation threshold and the measurement bandwidth was excessively large, it should not be difficult to achieve 10-mK temperature resolution in the future.

### *G. Stability*

Variations in acoustic sensitivity can be caused by changes in the optical power incident on the sensing film. Those caused by fluctuations in laser output power and launch efficiency can be readily compensated for by monitoring the optical power launched into the coupler using the monitor photodiode $P_L$ shown in Fig. 2 and suitably adjusting the laser drive current. Power fluctuations caused by fiber bending are potentially more troublesome because they are indistinguishable from changes in interferometer output that are due to environmentally induced phase bias shifts. However, it requires a fairly small bend radius (<1 cm) to produce a significant change in sensitivity (>10%), and, consequently, this was not found to be a limitation under normal operating conditions.

Acoustic sensitivity variations can also be caused by changes in phase bias caused by environmentally induced changes in the optical thickness of the sensing film such as those caused by water absorption [13], temperature changes (Section IV, F), or variations in hydrostatic pressure. The effect of these is to shift the phase bias away from quadrature. To compensate, it is necessary to retune the laser wavelength. However, this is a slow process with a thermally tuned laser diode (tens of seconds), and it is desirable that, under typical operating conditions, short-term environmentally induced changes in phase bias are small. To investigate this, a quadrature-set optical fiber

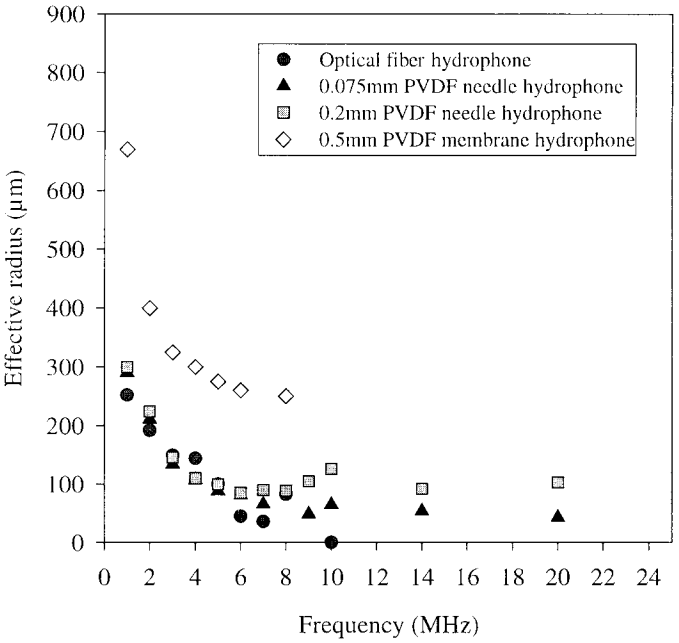


Fig. 8. Comparison of effective radii of PVDF needle and membrane hydrophones and the optical fiber hydrophone as a function of frequency.

hydrophone was positioned directly behind a PVDF membrane reference hydrophone in a water bath. Typical temperature excursions in the water bath over the measurement period were approximately 5°C. The peak-peak outputs of each device in response to a pulsed 3.5-MHz PZT transducer were compared every 30 s over a period of 20 h using a digitizing oscilloscope under PC control. The sensor output was divided by the output of the monitor photodiode $P_L$ to compensate for variations in laser launch power. An intrinsic sensor stability of <5% (limited by the experimental method) over 20 h was obtained.

In particular, it was observed that the response at the beginning of the measurement period when the sensor was first immersed in the water remained constant. This suggests that the change in film thickness caused by water absorption is negligible, a considerable improvement over PET sensing films in this respect [13]. Thus, any changes in acoustic sensitivity caused by environmentally induced phase shifts are likely to be those solely caused by temperature variations, and these need to be >10°C (Section IV) to produce significant sensitivity changes.

## V. Conclusions

A practical wideband optical fiber hydrophone has been developed that offers a realistic prospect of overcoming the shortcomings of piezoelectric PVDF measurement technology. In terms of acoustic performance, its principal advantage lies in the favorable active element size-sensitivity ratio it offers. In its present form, it can offer a lower directional sensitivity (<10 MHz) than that of a 0.075-mm PVDF needle hydrophone but with a detection sensitivity pressure comparable with that of a 0.2-mm PVDF hydrophone. It also has the advantage that it has the potential to self-monitor changes in calibration and to detect temperature changes. An important feature is that it can be fabricated by depositing the polymer film sensing element directly on to the end of the optical fiber. This enables a rugged sensor head to be batch-fabricated with good repeatability at low cost, thereby offering the prospect of a disposable hydrophone.

Among the possible applications are in situ exposimetry measurements of diagnostic and therapeutic medical ultrasound where the disposable nature of the hydrophone, its miniature, flexible probe-type configuration, low directional sensitivity, electrical passivity, and ability to measure temperature would be of benefit. Another application is the measurement and monitoring of CW low frequency, high power industrial ultrasound such as that employed in ultrasonic cleaning where small physical size to avoid disturbing standing wave patterns, the ability to withstand hostile environments, and low sensitivity to electrical interference are required. The concept may also be suited to detection applications such as acoustic emission studies, transmission ultrasound imaging, and photoacoustic and Hall effect imaging, all of which require a small aperture wideband receiver.

Future work is to concentrate on understanding more fully the effect of diffraction on the frequency and directional response in an effort to design a sensor head geometry that offers improved directional and frequency response characteristics. Additionally, the ability to make simultaneous temperature and acoustic pressure measurements is to be investigated further. It may also be appropriate to investigate alternative methods of interrogating the FP cavity. For example, low coherence methods [31] can offer a number of processing advantages over active homodyne. This is particularly true if quasi-static temperature variations are to be recovered or more rapid compensation for environmentally induced cavity length changes than can be obtained with a thermally tuned laser diode is required for use in hostile environments.

## Acknowledgment

The authors gratefully acknowledge Mr. D. Thomas, Dept. of Physics and Astronomy, UCL, for providing the aluminium coatings used in this work.

## References

[1] R. P. De Paula, J. H. Cole, and J. A. Bucaro, "Broad-band ultrasonic sensor based on induced optical phase shifts in single mode fibers," *IEEE J. Lightwave Technol.*, vol. LT-1, no. 2, pp. 390–393, 1983.

[2] R. P. De Paula, L. Flax, J. H. Cole, and J. A. Bucaro, "Single mode fiber ultrasonic sensor," *IEEE J. Quantum Electron.*, vol. QE-18, no. 4, pp. 680–683, 1982.

[3] N. E. Fisher, D. J. Webb, N. Pannell, D. A. Jackson, L. R. Gavrilov, J. W. Hand, L. Zhang, and I. Bennion, "Ultrasonic

hydrophone based on short in-fiber Bragg gratings," *Appl. Optics*, vol. 37, no. 34, pp. 8120–8128, 1998.
[4] S. Knudsen and K. Blotekjaer, "An ultrasonic fibre optic hydrophone incorporating a push-pull Sagnac interferometer," *IEEE J. Lightwave Technol.*, vol. 12, no. 9, pp. 1696–1700, 1994.
[5] H. Wen, D. G. Wiesler, A. Tveten, B. Danver, and A. Dandridge, "High sensitivity fiber optic ultrasound sensors for medical imaging applications," *Ultrason. Imag.*, vol. 20, pp. 102–112, 1998.
[6] J. Staudenraus and W. Eisenmenger, "Fibre-optic probe hydrophone for ultrasonic and shock-wave measurements in water," *Ultrasonics*, vol. 31, no. 4, pp. 267–273, 1993.
[7] D. P. Hand, S. Freeborn, P. Hodgson, T. A. Carolan, K. M. Quan, H. A. Mackenzie, and J.D.C. Jones, "Optical fiber interferometry for photoacoustic spectroscopy in liquids," *Optics Lett.*, vol. 20, no. 2, pp. 213–215, 1995.
[8] D. R. Bacon, "Primary calibration of ultrasonic hydrophones using optical interferometry," *IEEE Trans. Ultrason., Ferroelect., Freq. Contr.*, vol. 35, no. 2, pp. 152–161, 1988.
[9] C. Koch, "Measurement of ultrasonic pressure by heterodyne interferometry with a fibre tip sensor," *Appl. Optics*, vol. 38, no. 13, pp. 2812–2819, 1999.
[10] V. Wilkens and C. Koch, "Fiber optic multilayer hydrophone for ultrasonic measurement," *Ultrasonics*, vol. 37, pp. 45-49, 1999.
[11] P. C. Beard and T. N. Mills, "An optical fibre sensor for the detection of laser generated ultrasound in arterial tissues," *Proc SPIE*, vol. 2331, pp. 112–122, 1994.
[12] ——, "Extrinsic optical fibre ultrasound sensor using a thin polymer film as a low finesse Fabry-Perot interferometer," *Appl. Optics*, vol. 35, no. 4, pp. 663–675, 1996.
[13] P. C. Beard, F. Perennes, and T. N. Mills, "Transduction mechanisms of the Fabry Perot polymer film sensing concept for wideband ultrasound detection," *IEEE Trans. Ultrason., Ferroelect., Freq. Contr.*, vol. 46, no. 6, pp. 1575–1582, 1999.
[14] Y. Uno and K. Nakamura, "Pressure sensitivity of fiber-optic microprobe for high frequency ultrasonic field," *Jpn. J. Appl. Phys.*, vol. 38, part 1, no. 5B, pp. 3120–3123, May 1999.
[15] P. C. Beard and T. N. Mills, "A miniature optical fibre ultrasonic hydrophone using a Fabry Perot polymer film interferometer," *Electron. Lett.*, vol. 33, no. 9, pp. 801–803, 1997.
[16] A. J. Coleman, E. Draguioti, R. Tiptaf, N. Shotri, and J. E. Saunders, "Acoustic performance and clinical use of a fibreoptic hydrophone," *Ultrason. Med. Biol.*, vol. 24, no. 1, pp. 143–151, 1998.
[17] P. C. Beard, A. Hurrell, E. van den Elzen, and T. N. Mills, "Comparison of a miniature ultrasonic optical fibre hydrophone with PVDF hydrophone technology," *Proc. IEEE Ultrason. Symp.*, Sendai, Japan, pp. 1881–1884, 1998.
[18] H. Yasuda, *Plasma Polymerisation*. Academic Press, 1985.
[19] L. Holland, *Vacuum Deposition of Thin Films*, London: Chapman and Hall Ltd., 1970.
[20] J. F. Dorighi, S. Krishnaswamy, and J. D. Achenbach, "Stabilisation of an embedded fibre optic Fabry-Perot sensor for ultrasound detection," *IEEE Trans. Ultrason., Ferroelect., Freq. Contr.*, vol. 42, no. 5, pp. 820–824, 1995.
[21] R. A. Smith and D. R. Bacon, "A multiple frequency hydrophone calibration technique," *J. Acoust. Soc. Amer.*, vol. 87, no. 5, pp. 2231–2242, 1990.
[22] R. C. Preston, D. R. Bacon, A. J. Livett, and K. Rajendran, "PVDF membrane hydrophone performance properties and their relevance to the measurement of the acoustic output of medical ultrasound equipment," *J. Phys. E:Sci. Instrum.*, vol. 16, pp. 786–796, 1983.
[23] P. A. Lewin, "Practical implementations and technology of measurement devices," in *Ultrasonic Exposimetry*, M. C. Ziskin and P. A. Lewin, Eds. Boca Raton, FL: CRC Press, 1993, p. 195.
[24] S. P. Robinson, "A comparison of the frequency response of membrane and needle probe PVDF hydrophones," in *Proc. Phys. Med. Ultrasound II*, Rep. no. 57, IPSM, D. G. Evans and K. Martin, Eds. pp. 79–86, 1987.
[25] D. S. Jones, "The scattering of a scalar wave by a semi infinite rod of circular cross section," *Phil. Trans. R. Soc.*, vol. A257, pp. 499–528, Apr. 1955.
[26] B. Fay, G. Ludwig, C. Lankjaer, and P. A. Lewin, "Frequency response of PVDF needle-type hydrophones," *Ultrason. Med. Biol.*, vol. 20, no. 4, pp. 361–366, 1994.
[27] M. R. Smith and H. R. Gallantree, "PVDF membrane hydrophones: An ultrasonic characterisation tool," Great Baddow, Essex, UK: GEC-Marconi, 1993, p. 6.
[28] P. M. Morse and U. K. Ingard, *Theoretical Acoustics*. New York: McGraw-Hill, 1968, p. 381.
[29] G. Harris, "Hydrophone measurements in diagnostic ultrasound fields," *IEEE Trans. Ultrason., Ferroelect., Freq. Contr.*, vol. 35, no. 2, pp. 87–101, Mar. 1988.
[30] P. C. Beard, F. Perennes, E. Draguioti, and T. N. Mills, "An optical fibre photoacoustic-photothermal probe," *Optics Lett.*, vol. 23, no. 15, pp. 1235–1237, 1998.
[31] D. A. Jackson and J.D.C. Jones, "Interferometers," in *Optical Fibre Sensors: Systems and Applications*, vol. 2, B. Culshaw and J. Dakin, Eds. Norwood, MA: Artech House, 1989, ch. 1, pp. 357–359.

**Paul Beard** received a degree in Physics from University College London, UK, in 1987 and a PhD in Medical Physics in 1996 also from University College London. Between 1989 and 1992, he worked for Marconi Underwater Systems Ltd., UK, on the development of underwater interferometric optical fiber hydrophone arrays and magnetic sensors. Since then, he has been employed in the Department of Medical Physics and Bioengineering at University College London, where he is Senior Research Fellow. His current research interests include photoacoustic spectroscopy and imaging for biomedical applications and the development of optical fiber ultrasound sensing techniques.

**Andrew M. Hurrell** was born in Ashford, Kent, England, on January 12, 1972. He received the B.Sc. Degree in Physics and Modern Acoustics at the University of Surrey in 1994. He is currently pursuing his Ph.D. part-time at the University of Bath. From 1994 to 1996, he was a member of the Acoustic Materials Team at the Defense Research Agency (Holton Heath). In 1996, he joined Precision Acoustics Ltd., Dorchester, as Transducer Design Engineer. His current interests include design and construction of hydrophones/hydrophone arrays and the use of finite difference techniques to model acoustic phenomena.

**Tim N. Mills** was born in the UK. He received the B.Sc.(Eng) and Ph.D. degrees from the Imperial College of Science, Technology and Medicine, London, England. Since 1980, he has worked in the Department of Medical Physics and Bioengineering, University College London, and UCL Hospitals NHS Trust, London, UK conducting research into medical laser applications, endoscopic instrumentation, and optical fiber sensors. He presently heads the department's Medical Lasers and Endoscopy section. He is a member of the Institute of Physics and Engineering in Medicine.